https://doi.org/10.5194/egusphere-2024-3923
Preprint. Discussion started: 27 March 2025

Modeling Regional Production Capacity Loss Rates Considering Response Bias: Insights from a Questionnaire Survey on Zhengzhou Flood

Lijiao Yang[1], Yan Luo[1], Zilong Li[2], and Xinyu Jiang[3]

[1]School of Management, Harbin Institute of Technology, Harbin, 150001, China
[2]Control and Simulation Center, Harbin Institute of Technology, Harbin, 150080, China
[3]School of Government, Nanjing University, Nanjing, 210093, China

Correspondence: Xinyu Jiang (jxy119@nju.edu.cn)

Abstract. Flood disasters in specific regions not only cause physical damage but also disrupt the production and operations of enterprises, making economic system more vulnerable. Assessing production capacity loss rate (PCLR) in enterprises is crucial for quickly evaluating disaster losses. However, PCLR in enterprises is difficult to measure through physical damage. On-site investigations offer a compromise method, but inconsistencies between respondents and investigators in understanding production capacity may result in response bias. Therefore, this study employed the vulnerability curve method for categorizing damage states to divide PCLR into different damage states and constructed exceedance probability curves to mitigate response bias. Then, this study utilized distribution function fitting to calculate the expectation of loss rate for each state, and finally integrated the probabilistic information with the expectation of loss rate under each state to construct PCLR curves. The proposed methodology is realized by the questionnaire data from the "7.20" extreme flooding event in Zhengzhou, Henan. We found that when the inundation depth is less than 80 cm, wholesale and retail trade sector suffers the greatest losses; however, when the inundation depth exceeds 80 cm, we should pay more attention to manufacturing sector. Monte Carlo simulation (MCS) established the prediction intervals of PCLR curves, offering an alternative for PCLR. This study effectively accounts for response bias, providing input conditions for assessing ripple losses.

1 Introduction

The impact of natural disasters has become a significant global concern. In 2023, the Emergency Event Database (EM-DAT) reported 399 natural disasters worldwide. These disasters affected 93.1 million people and resulted in approximately USD 202.7 billion in economic losses. Of these events, floods accounted for 41.10% of the total incidents (EMDAT, 2024), significantly affecting economic growth (IPCC, 2023). Consequently, an amount of literature has emerged, employing numerous model-based and empirical methods to explore the macro and micro-economic impacts of natural disasters (Hallegatte et al., 2013; Koks et al., 2016; Botzen et al., 2019). At the macro-economic level, researchers widely utilize Input-Output (I-O) models (Okuyama and Santos, 2014; Koks and Thissen, 2016; Lenzen et al., 2019), Computable General Equilibrium (CGE) models (Kajitani and Tatano, 2018; Gertz et al., 2019), and integrated assessment models (Carrera et al., 2015; Koks et al., 2015) to

https://doi.org/10.5194/egusphere-2024-3923
Preprint. Discussion started: 27 March 2025

quantify the economic effects of natural disasters. These methods allow a comprehensive analysis of the overall impact on national and regional economies. At the micro-economic level, methods for assessing business resilience have been developed, primarily focusing on resistance and recovery (Liu et al., 2024). However, due to the different focuses of the two types of models, and the difficulties in obtaining business data caused by confidentiality concerns, micro-level assessment methods for individual enterprises are often difficult to integrate with macro-level economic assessment methods for estimating overall regional industry losses.

Estimating regional industry losses is crucial for understanding the vulnerability of local industries and facilitating post-disaster recovery. As previously mentioned, macro-economic models such as IO (Jiang et al., 2023) and CGE (Yang et al., 2023) are designed to capture complex and higher-order impacts (Tatano and Kajitani, 2022). However, these models require specific inputs to function effectively. Industry losses are commonly considered a fundamental input for macroeconomic models when modeling supply shocks. Recently, production capacity loss rate (PCLR) has been proposed as a competing input for these models, relying on estimated outputs from vulnerability curves (Kajitani and Tatano, 2014; Liu et al., 2022a; Jiang et al., 2015). These curves can be rapidly estimated if accurate data is available, especially in the engineering field. Generally, this method can be insightful when PCLR data is accessible. However, it still faces challenges due to response bias, particularly during extreme flooding events.

Response bias stems from multiple factors, including personal perception biases (Liu et al., 2022b), memory inaccuracies (Tan et al., 2023), and emotional influences (Cai and Wei, 2020). Empirical evidence, as advocated at the 2015 Sendai Conference, highlights the importance of collecting data directly from disaster sites (UNDRR, 2015). Borga et al. (2019) stressed that post-flood surveys should begin immediately after the event to prevent potential erasure of site evidence, which is a critical reference for government recovery efforts. According to Cabrera et al. (2024), the empirical approach is most effective for deriving realistic fragility curves as it relies on actual damage data. However, the success of these actions relies on accurate data estimations. Unlike the objectivity of physical indicators such as ground deformation (Choi et al., 2004), relative displacement between the crown of arch and the inverted arch (Andreotti and Lai, 2019), volumetric water content (Vergeynst et al., 2015) and accident events (Yang et al., 2020), estimating PCLR relies on the subjective judgment of enterprise managers, resulting in significant uncertainty. Moreover, PCLR collected is often not continuous loss data that can be estimated using regression methods (Zentner et al., 2017). Consequently, while some researchers either assume loss rate data or simply analyze the relationship between hazard intensity and loss, this approach can overestimate or underestimate the actual loss, thereby amplifying or attenuating the risk. This highlights an urgent need for more reliable methods and data in PCLR estimation, including categorizing damage states, which is essential for understanding loss characteristics across different damage states.

Categorizing damage states based on loss rate data is a desirable approach in existing literature on earthquakes and engineering (Baker, 2015; Padgett and DesRoches, 2008; Nguyen et al., 2024). Prasad and Banerjee (2013) classified bridge damage into four states and established probability curves for bridge failure at specific seismic intensities using these classifications. Andreotti and Lai (2019) pointed out that the loss mechanisms vary under different damage states, and the damage index of tunnel structures after an earthquake shows high variability except in the no-damage state. The economic impact of floods is

https://doi.org/10.5194/egusphere-2024-3923
Preprint. Discussion started: 27 March 2025

more complex, and it is worth noting that there are significant differences in loss mechanisms across different damage states. Therefore, classifying damage states is essential for better understanding loss characteristics in different situations.

Motivated by the gaps mentioned above, we propose a response-bias-tolerant framework that accounts for response bias to estimate PCLR curves. Firstly, we conduct a questionnaire survey and classify damage states, and then utilize the exceedance probability curve model to develop exceedance probability curves. This approach helps us handle data affected by response bias and determine the likelihood of different damage states at different inundation depths. Secondly, we fit PCLR to a probability distribution within each damage state, from which we derive the expectation of loss rate for further analysis. Finally, by integrating the expectation of loss rate with their associated probabilities under each damage state, we provide a more adaptable assessment of the mean PCLR for businesses in the post-disaster phase. Furthermore, based on Yang et al. (2016), we extend our analysis of PCLR curves by employing Monte Carlo simulation (MCS) to generate prediction intervals of PCLR curves, and analyzing the rate of change of PCLR.

The remainder of this study is organized as follows. Section 2 illustrates the overall framework for estimating the mean PCLR. Section 3 presents a case study of the 2021 Zhengzhou flood. Section 4 offers the results and a discussion on the implementation and improvement of the proposed method, along with policy recommendations. Finally, the conclusions are summarized in Section 5.

2 Methodology

A methodological framework was proposed to construct PCLR curves. Firstly, we categorize damage states of PCLR affected by response bias, and then construct exceedance probability curves using exceedance probability curve model. These curves form the foundation for further probability curve extrapolation. Secondly, this study fits distribution functions to PCLR for different damage states, facilitating the calculation of the expectation of loss rate under each damage state. Finally, PCLR curves are constructed by integrating probability curves with the expectation of loss rate under each damage state. These methodological steps provide insights for prioritizing sectors based on their risk, as shown in the framework presented in Fig. 1.

2.1 Exceedance probability curve model

Exceedance probability curve model is widely applied in civil and structural engineering for assessing structural reliability and seismic response (Burton et al., 2016; Hariri-Ardebili and Saouma, 2016). It simulates random processes to generate probability curves that gauge the likelihood of extreme structural reactions for risk assessment (Shinozuka et al., 2000; Torbol and Shinozuka, 2012; Karmakar et al., 2015). This method, traditionally used in engineering, has recently been applied to the study of functional damage, like reduction in production capacity (Nakano et al., 2013).

https://doi.org/10.5194/egusphere-2024-3923
Preprint. Discussion started: 27 March 2025

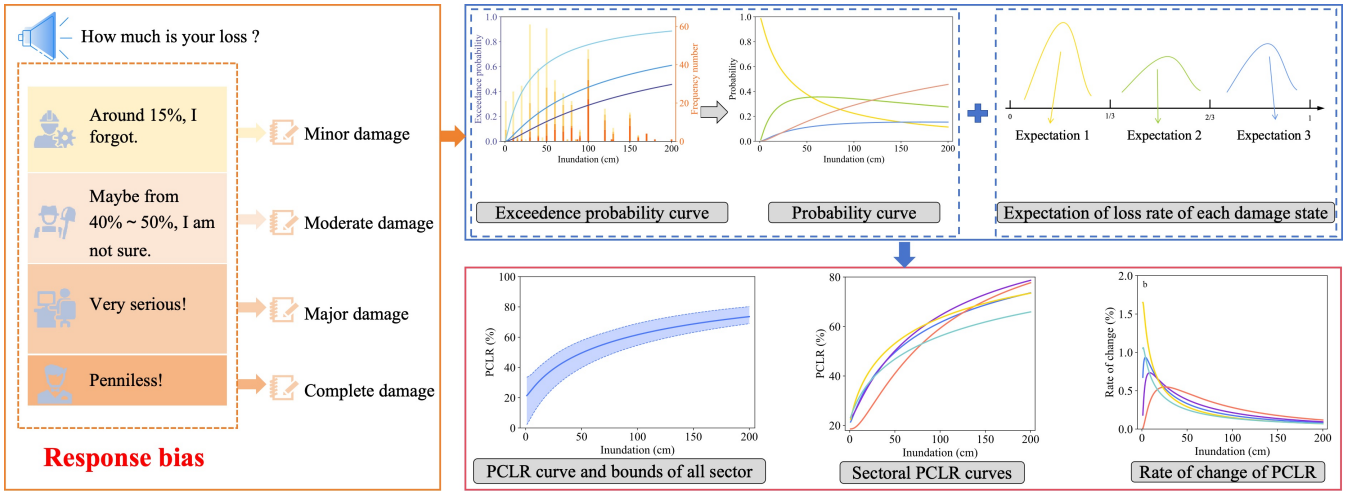

Figure 1. An overview of the framework for constructing PCLR curves.

In this study, we assume that the probability of exceeding a damage state is a function of inundation depth h represented as a two-parameter Lognormal distribution function, given in Eq. (1):

$$F_\omega(h;\mu_\omega,\sigma) = \Phi\left(\frac{\ln h - \mu_\omega}{\sigma}\right). \tag{1}$$

$F_\omega(h;\mu_\omega,\sigma)$ represents the probability of exceeding a certain damage state; $\Phi(\cdot)$ is the cumulative distribution function (CDF) of the standard normal distribution; μ_ω and σ are the mean and standard deviation of Lognormal distribution, corresponding to "exceeding minor damage", "exceeding moderate damage", and "exceeding major damage", differentiated by ω.

Utilizing three damage curves, we can determine four distinct damage states d_j, namely minor damage (d_0), moderate damage (d_1), major damage (d_2), and complete damage (d_3). $P_j(h)$ denotes the probability of being in damage state d_j when the inundation depth is h. Subsequently, the probabilities for these four damage states, conditional upon the inundation depth h, are expressed in Eq. (2):

$$\begin{aligned} P_0(h) &= 1 - F_1(h;\mu_1,\sigma), \\ P_1(h) &= F_1(h;\mu_1,\sigma) - F_2(h;\mu_2,\sigma), \\ P_2(h) &= F_2(h;\mu_2,\sigma) - F_3(h;\mu_3,\sigma), \\ P_3(h) &= F_3(h;\mu_3,\sigma). \end{aligned} \tag{2}$$

The parameters (μ_ω,σ) are estimated by maximizing a likelihood function, expressed in Eq. (3):

$$L(\mu_1,\mu_2,\mu_3,\sigma) = \prod_{i=1}^{N}\prod_{j=0}^{3}[P_j(h_i)]^{\delta_{ij}}, \tag{3}$$

https://doi.org/10.5194/egusphere-2024-3923
Preprint. Discussion started: 27 March 2025

where $\delta_{ij} = 1$ if damage states d_j occur for the enterprise i subjected to $h = h_i$, and $\delta_{ij} = 0$, otherwise. The estimation of parameters μ_ω and σ using the maximum likelihood method can be achieved by solving the following equation:

$$\frac{\partial \ln L(\mu_1, \mu_2, \mu_3, \sigma)}{\partial \mu_\omega} = \frac{\partial \ln L(\mu_1, \mu_2, \mu_3, \sigma)}{\partial \sigma} = 0 \qquad (\omega = 1, 2, 3). \tag{4}$$

Furthermore, to evaluate the assumption that the inundation depth can serve as a variable of the decline in production capacity immediately following a catastrophe, the likelihood ratio test is utilized to check the alternative hypothesis. The null hypothesis is that the probabilities of occurrence of damage states occur equally in this case study.

2.2 Distribution function fitting for PCLR in each damage state

In this study, we employ distribution function fitting to model PCLR under different damage states, aiming to estimate the expectation of loss rate. Distribution function fitting involves selecting a probability distribution function that best describes the observed data (Heo et al., 2022). Common distributions include Weibull, Lognormal, Gamma and Logistic (Moccia et al., 2021; Lima et al., 2021; Zhang et al., 2021). Goodness-of-fit tests, such as Akaike Information Criterion (AIC) and Bayesian Information Criterion (BIC), are utilized to evaluate the model's fit. The distribution that fits best is used for further analysis and predictions.

The Weibull distribution with shape parameter $k > 0$ and scale parameter $\lambda > 0$ has density given by:

$$f_{\mathrm{wb}}(x) = k\lambda^{-k} x^{k-1} \exp(-\lambda^{-k} x^k) \tag{5}$$

for $x > 0$, and the expectation of loss rate is:

$$E_{\mathrm{wb}} = \lambda \Gamma\left(1 + \frac{1}{k}\right), \tag{6}$$

where Gamma function is $\Gamma(z) = \int_0^{+\infty} u^{z-1} \exp(-u) \mathrm{d}u$ on $z > 0$.

The Lognormal distribution has density given by:

$$f_{\ln}(x) = \frac{1}{x\sigma\sqrt{2\pi}} \exp\left(-\frac{(\ln x - \mu)^2}{2\sigma^2}\right), \tag{7}$$

where μ and σ are the mean and standard deviation of the logarithm. The expectation of loss rate is:

$$E_{\ln} = \exp\left(\mu + \frac{\sigma^2}{2}\right). \tag{8}$$

The Gamma distribution with shape parameter α and scale parameter β has density given by:

$$f_{\mathrm{gm}}(x) = \frac{x^{\alpha-1}}{\beta^\alpha \Gamma(\alpha)} \exp\left(-\frac{x}{\beta}\right). \tag{9}$$

The expectation of loss rate is:

$$E_{\mathrm{gm}} = \alpha\beta. \tag{10}$$

https://doi.org/10.5194/egusphere-2024-3923
Preprint. Discussion started: 27 March 2025

The Logistic distribution with location parameter ν and scale parameter τ has density given by:

$$f_{\mathrm{ls}}(x) = \frac{\exp((x-\nu)/\tau)}{\tau(1+\exp((x-\nu)/\tau))^2}. \tag{11}$$

The expectation of loss rate is:

$$E_{\mathrm{ls}} = \nu. \tag{12}$$

2.3 Sector-specific estimation of PCLR curves

After estimating probability curves and the expectation of loss rate for each damage state, we can estimate the mean PCLR for each sector by generating PCLR curves. The estimation of enterprise's mean PCLR can be expressed as:

$$Lr(h) = \sum_{j=0}^{3} m_j P_j(h), \tag{13}$$

$Lr(h)$ represents the mean PCLR estimates of the enterprise. m_j is chosen as the expectation of the optimal distribution of loss rate under damage state d_j (one of E_{wb}, E_{ln}, E_{gm}, E_{ls}); $P_j(h)$ is the probability under each damage state obtained using exceedance probability curve model.

2.4 Prediction intervals of PCLR curves using MCS

Monte Carlo simulation is employed to solve problems characterized by various uncertainties and has found widespread application across numerous fields (Christensen et al., 2024; Asche et al., 2021; Goda et al., 2020). By creating multiple simulated scenarios, it approximates the distribution of a specific outcome (Sun et al., 2022). The model's iterative estimates generate a dataset of possible outcomes, which, when aggregated, define the range of the true outcome with a specified probability. In this study, we employ MCS to generate prediction intervals for PCLR curves in different sectors. Specifically, we draw random numbers from the best-fit distribution selected in Section 2.2. For minor damage, random numbers are drawn from the range (0, 1/3); for moderate damage from [1/3, 2/3); and for major damage from [2/3, 1). Then, these random numbers, combined with the probabilities of the damage states occurring, generate several datasets. This process is repeated 1000 times, stabilizing prediction intervals that define the upper and lower bounds of PCLR curves. These intervals quantify the uncertainty of the outcome in PCLR estimates and support the flexible allocation of government post-disaster recovery funds.

3 3.Case study: the "7.20" flooding event in Zhengzhou

3.1 Overview of the "7.20" Zhengzhou flooding event

Zhengzhou City, located in central China (Fig. 2), is the provincial capital of Henan Province and a major hub for commerce and industry. The city hosts numerous local businesses that significantly contribute to its economic development. By the end of 2023, Zhengzhou had a permanent urban population of approximately 13 million and a substantial gross domestic product.

https://doi.org/10.5194/egusphere-2024-3923
Preprint. Discussion started: 27 March 2025

In July 2021, Henan was struck by heavy rainfall that drew the attention of many scholars (Dong et al., 2022; Peng and Zhang, 2022; Lv et al., 2024). Zhengzhou's losses were 40.9 billion yuan, accounting for 34.1% of the total loss for the province. This catastrophic flooding caused widespread disruptions including production stoppages, supply chain breakdowns, infrastructure damage, and financial losses for local enterprises, severely affecting their operations and employees.

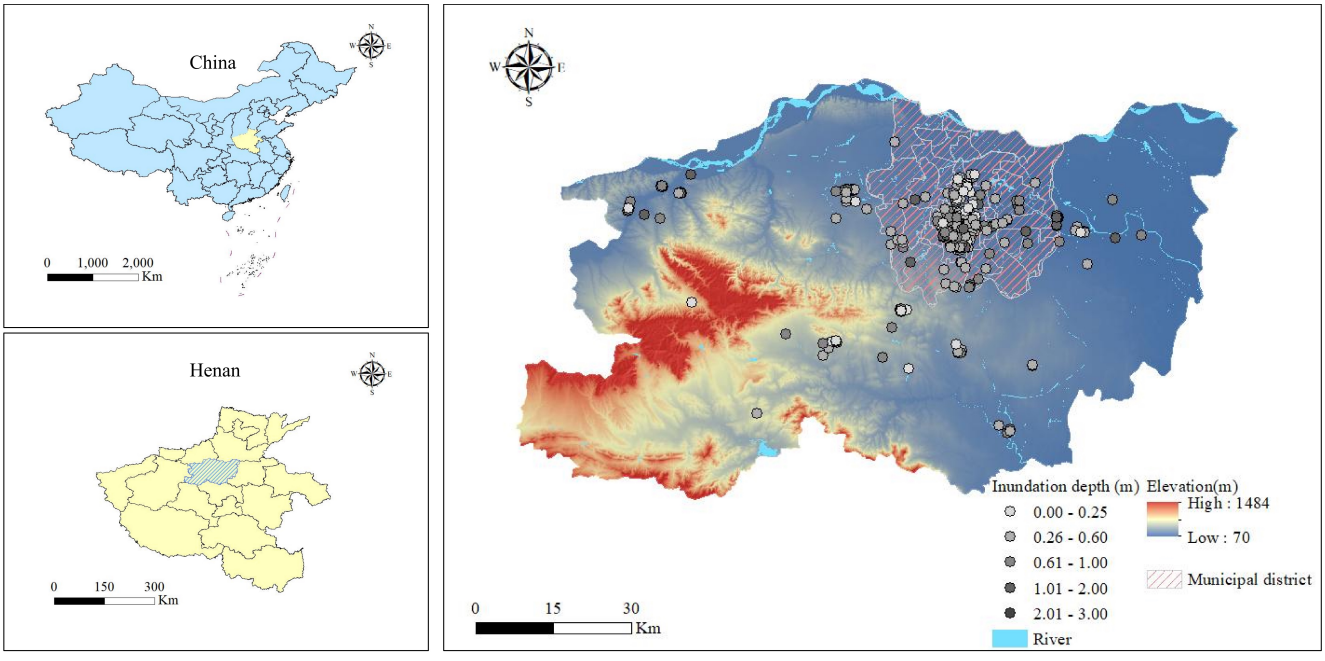

Figure 2. Study area and spatial distribution of enterprise samples.

3.2 Data collection

To collect PCLR of enterprises affected by the flood, we conducted questionnaire surveys and in-depth interviews from April 19th to May 4th, 2023. We focused on disaster-stricken enterprises in Zhengzhou, and collected data on PCLR, local inundation depths, the duration of flood impacts and so on. A total of 424 valid samples were gathered. These samples were primarily distributed within the administrative districts of Zhengzhou City. Based on this data, this study categorized and summarized the samples, of which 148 belonged to manufacturing sector, 68 to accommodation and catering sector, 137 to wholesale and retail trade sector, and 71 to other sectors.

3.3 Measurement of loss: PCLR of different sectors

PCLR refers to the direct impact on enterprises following a flood due to multiple factors, resulting in a rapid decrease or loss in their original production capacity (Kajitani and Tatano, 2014). On one hand, there are direct losses caused by the destruction of tangible assets (Hung et al., 2022) such as factory equipment, warehouses, and inventories of raw materials; on the other

https://doi.org/10.5194/egusphere-2024-3923
Preprint. Discussion started: 27 March 2025

Table 1. Categories of damage states.

Damage state	PCLR
Minor damage	(0, 1/3)
Moderate damage	[1/3, 2/3)
Major damage	[2/3, 1)
Complete damage	1

hand, there are indirect losses resulting from damage to essential infrastructure (Wei et al., 2015) like power supply, water supply, and transportation networks, injuries to employees who are unable to work or evacuated (Brusset et al., 2023), as well as significant market demand shifts (Kaur et al., 2020).

As demonstrated by the framework for constructing PCLR curves, the collected PCLR is often inaccurate due to response bias. For instance, victims may provide only a range for PCLR or a brief description of the damage. Therefore, further data processing is required. In this paper, PCLR is categorized by different damage states. These states are: minor, moderate, major, and complete damage, as illustrated in Table 1.

4 Results

Exceedance probability curve model is utilized to estimate exceedance probability of each damage state at a given inundation depth h. These estimates are first visualized as exceedance probability curves, which are then transformed into probability curves. This section presents the estimated probability curves conditional on the different PCLR across sectors following the "7.20" Zhengzhou flooding event. Next, by selecting appropriate distribution functions, the expectation of loss rate under each damage state is calculated. Subsequently, PCLR curves are estimated by integrating probability curves with the expectation of loss rate. Finally, the prediction intervals of PCLR curves and the rate of change in PCLR are estimated.

4.1 Estimated probability curves across sectors

4.1.1 Estimated exceedance probability curves across sectors

By employing exceedance probability curve model, we constructed exceedance probability curves for four distinct sectors. This study presents the fitting parameters for the model, as shown in Table 2. Additionally, this table presents values (χ^2) of likelihood ratio tests. The critical value at a significance level of $p = 0.005$ with four degrees of freedom is 14.860. The smallest estimated value among the four sectors is 15.393. Thus, it can be inferred that the alternative hypothesis (that inundation depth can be used to estimate the decline in production capacity) is supported for all sectors at a significance level of 0.5%.

Fig. 3 illustrates exceedance probability curves for each sector. Varying shades of blue depict the exceedance probability under different damage states. The darkest shade represents the probability of exceeding major damage, the lightest shade

https://doi.org/10.5194/egusphere-2024-3923
Preprint. Discussion started: 27 March 2025

represents the probability of exceeding minor damage, and the medium shade represents the probability of exceeding moderate damage. The bar charts show the sample distribution in each damage state under different inundation depth conditions.

Analysis of Table 2 and Fig. 3 reveals differences in the exceedance probabilities of damage states across sectors. Specifically, the exceedance probabilities of major damage (complete damage) are significantly higher in the deep water sectors for manufacturing and accommodation and catering sectors compared to wholesale and retail trade sector. In addition, the exceedance probabilities of minor damage (moderate, major, and complete damage) are higher in the shallow water sectors for manufacturing sector compared to both accommodation and catering sector and wholesale and retail trade sector.

Table 2. Fitting parameters of exceedance probability curves.

Parameter	All sectors N=424	Manufacturing N=148	Accommodation and catering N=68	Wholesale and retail trade N=137	Other sectors N=71
μ_1	3.425	3.328	4.050	3.256	3.722
	[0.107]	[0.153]	[0.173]	[0.232]	[0.322]
μ_2	4.862	4.804	4.792	4.666	5.305
	[0.140]	[0.178]	[0.242]	[0.268]	[0.523]
μ_3	5.467	5.154	5.090	5.585	6.348
	[0.185]	[0.210]	[0.299]	[0.403]	[0.738]
σ	1.555	1.177	1.072	1.870	1.946
	[0.161]	[0.169]	[0.287]	[0.389]	[0.488]
$\log L_1$	−476.127	−153.740	−73.719	−166.395	−68.546
$\log L_0$	−532.644	−182.289	−81.416	−179.249	−78.790
χ^2	113.034	57.100	15.393	25.708	20.487

Note: Numbers in parentheses are standard deviations of the estimated parameter values.

4.1.2 Estimated probability curves across sectors

For further analysis, the exceedance probabilities were transformed into probabilities for different damage states, corresponding to the areas enclosed by the various exceedance probability curves depicted in Fig. 4. The yellow, green, blue, and red lines represent the probabilities of minor, moderate, major, and complete damage, respectively. Within the inundation depth range of 1 to 200 cm, the probability of manufacturing sector experiencing a moderate damage state is roughly equivalent to that of a complete damage state. In other sectors, the likelihood of minor damage state is generally comparable to that of moderate damage state, while accommodation and catering sector, as well as wholesale and retail trade sector, are more prone to both minor and complete damages. Due to the limited samples of major damage, the probability of a major damage state occurring under any inundation depth remains relatively low, never dominating the spectrum of damage states.

https://doi.org/10.5194/egusphere-2024-3923
Preprint. Discussion started: 27 March 2025

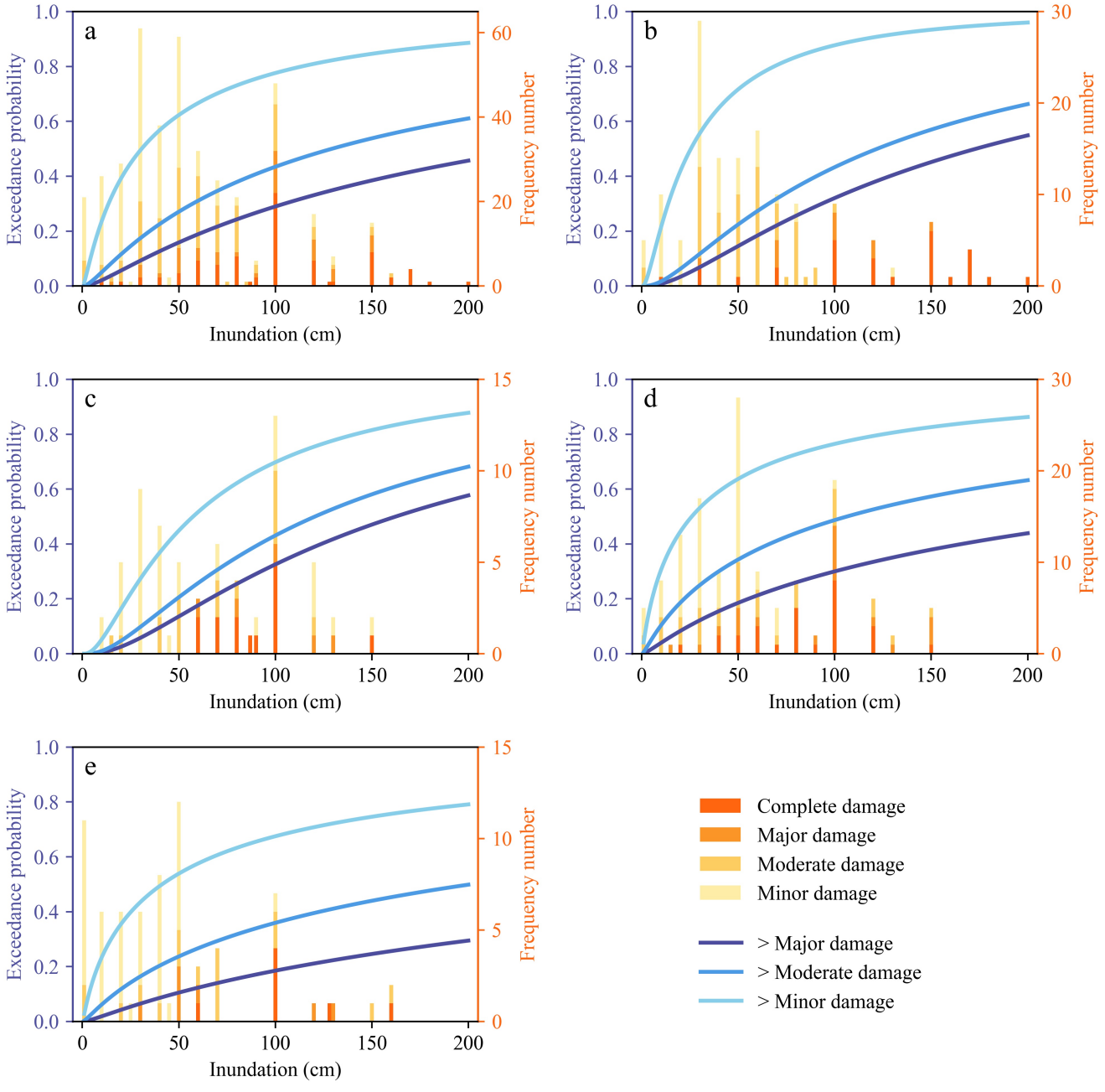

Figure 3. Exceedance probability curves of different sectors. (a) All sectors; (b) manufacturing; (c) accommodation and catering; (d) wholesale and retail trade; (e) other sectors.

https://doi.org/10.5194/egusphere-2024-3923
Preprint. Discussion started: 27 March 2025

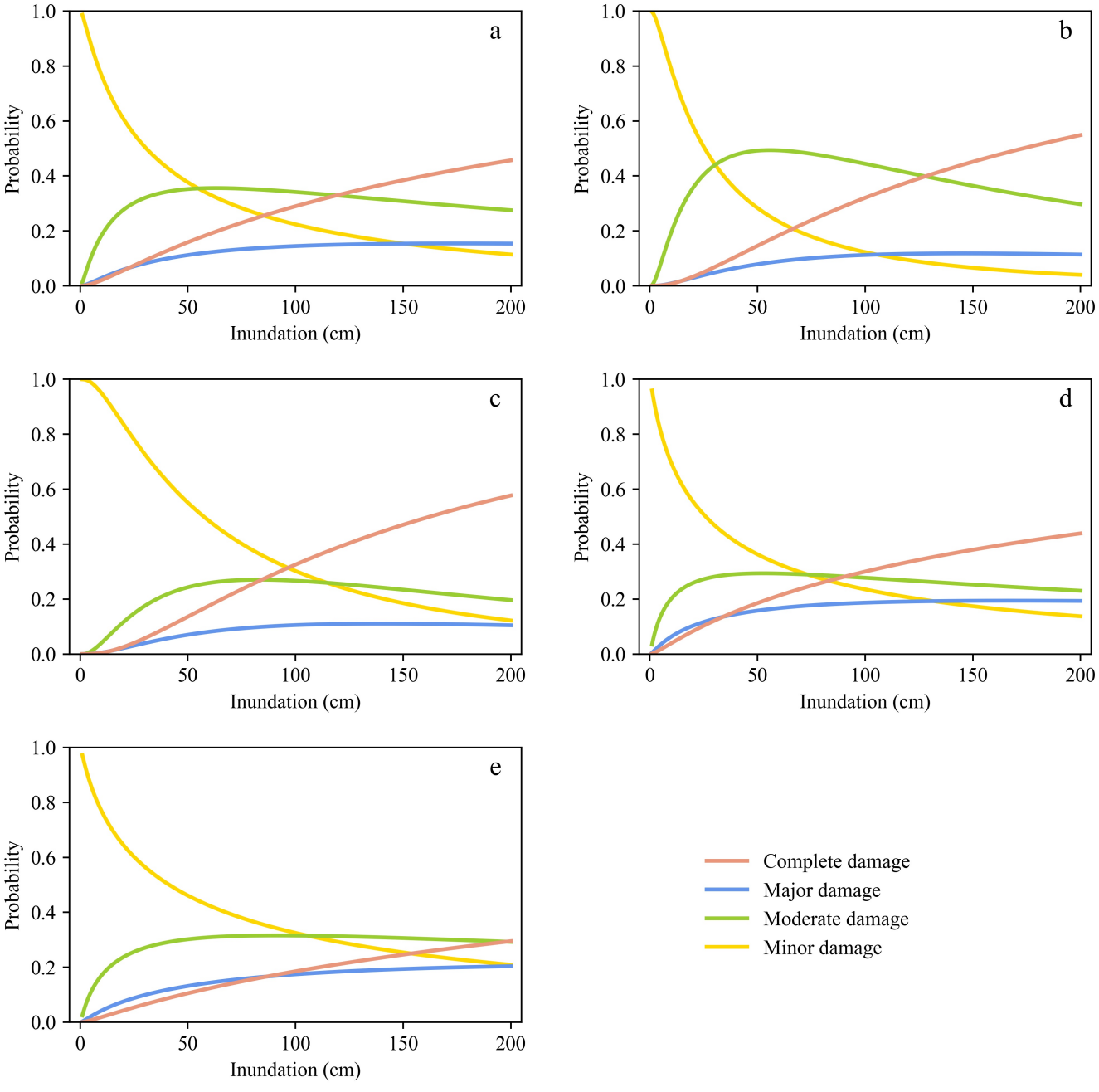

Figure 4. Probability curves of different sectors. (a) All sectors; (b) manufacturing; (c) accommodation and catering; (d) wholesale and retail trade; (e) other sectors.

https://doi.org/10.5194/egusphere-2024-3923
Preprint. Discussion started: 27 March 2025

4.2 Expectation of loss rate under each damage state

4.2.1 Distribution function fitting of PCLR

According to AIC and BIC, different functions, Weibull, Lognormal, Gamma, and Logistic, are selected as the best fit for various sectors under different damage states. These statistical criteria are utilized to evaluate the suitability and performance of each distribution function in representing the observed data. By analyzing AIC and BIC, we can identify which distribution function minimized information loss while balancing model complexity and fit. The goodness-of-fit values can be found in Table 3.

Table 3. Goodness-of-fit values for various distribution functions.

State \ Sector / Function		All sectors	Manufacturing	Accommodation and catering	Wholesale and retail trade	Other sectors
Minor	Weibull	−339.228;−332.809⋆	−109.019;−105.116⋆	−67.335;−64.283⋆	-83.235;−79.184	−88.516;−85.089⋆
	Lognormal	−236.769;−230.350	−86.679;−82.777	−62.847;−59.795	−51.021;−46.970	−74.065;−70.638
	Gamma	−299.498;−293.079	−96.286;−92.384	−65.583;−62.530	−74.196;−70.145	−80.255;−76.828
	Logistic	−338.316;−331.897	−105.043;−101.141	−61.344;−58.291	−86.573;−82.522⋆	−84.316;−80.889
Moderate	Weibull	−262.665;−257.024	−112.840;−108.719	−28.398;−26.982	−80.027;−76.916⋆	−33.016;−31.471
	Lognormal	−270.557;−264.916⋆	−121.501;−117.381⋆	−28.820;−27.404	−79.133;−76.022	−33.555;−32.010
	Gamma	−270.348;−264.707	−120.292;−116.171	−28.913;−27.497⋆	−79.749;−76.639	−33.661;−32.116⋆
	Logistic	−257.536;−251.895	−112.003;−107.882	−27.666;−26.250	−78.936;−75.825	−32.641;−31.096
Major	Weibull	−104.976;−101.549	−27.851;−27.246	−5.982;−6.763⋆	−48.521;−46.632	−21.228;−21.336⋆
	Lognormal	−106.267;−102.840	−29.663;−29.057	−5.959;−6.740	−50.741;−48.852	−19.645;−19.753
	Gamma	−106.500;−103.073⋆	−29.715;−29.110	−5.965;−6.746	−50.774;−48.886	−19.717;−19.825
	Logistic	−105.634;−102.207	−32.008;−31.403⋆	−5.286;−6.068	−51.201;−49.313⋆	−19.138;−19.246

Note: The values separated by semicolons are the AIC and BIC values, respectively; the asterisk indicates the best fit.

4.2.2 Estimation of expectation of loss rate under various damage states

In Section 4.2.1, the optimal distribution functions for PCLR under various damage states are selected. Subsequently, the expectation of loss rate under each damage state can be obtained. It is calculated using Eq. (6), Eq. (8), Eq. (10) or Eq. (12) and is presented in Table 4.

https://doi.org/10.5194/egusphere-2024-3923
Preprint. Discussion started: 27 March 2025

Table 4. Expectation of loss rate under various damage states.

State \ Sector	All sectors	Manufacturing	Accommodation and catering	Wholesale and retail trade	Other sectors
Minor damage	21.001	23.014	18.582	21.033	22.448
Moderate damage	47.449	46.281	47.558	48.973	48.124
Major damage	80.975	80.000	80.106	79.693	86.634

Note: Unit %.

4.3 Analysis of PCLR curves across sectors

4.3.1 Prediction intervals of PCLR curves using MCS

Utilizing probability curves from Section 4.1.2 and the expectation of loss rates estimated for each sector under different damage states in Section 4.2.2, PCLR curves are estimated using Eq. (13) and illustrated as solid lines in Fig. 5. Generally, PCLR values for each sector demonstrate a logarithmic increase with inundation depth. At lower inundation depths, the loss increases more rapidly; however, as inundation depth rises, the loss tends to stabilize. This highlights the nonlinear characteristics of loss growth across sectors at varying inundation depths.

Additionally, the model indicates that losses can occur even without any inundation. PCLR can reach up to 20% without direct floodwater damage. This primarily results from indirect factors that disrupt business operations: (1) Supply chain disruption: flooding can block transportation routes (Yin et al., 2016), delaying the delivery of raw materials and finished goods. (2) Workforce availability: Damaged roads and public transit systems can stop employees from commuting, affecting workforce presence. (3) Precautionary shutdowns: Businesses may temporarily close to reduce risks, which impacts production capacity despite being short-term. (4) Infrastructure interruptions: Temporary disruptions of essential services, such as electricity and water (Kayaga et al., 2021), cause operational delays. (5) Customer demand: During a disaster, demand drops as people prioritize safety and essential needs, reducing sales and affecting production.

To obtain the prediction intervals for PCLR curves across sectors, MCS is employed. These intervals are shown in dashed lines in Fig. 5. As inundation depth increases, these lines become tighter, indicating less variability in the PCLR estimates. This trend is crucial as it provides more reliable estimates at higher inundation depths. Narrower intervals assist decision-makers in making quicker and more informed decisions since potential losses are more predictable. Improved predictability aids in efficient resource allocation, emergency response planning, and risk mitigation. By understanding these intervals, stakeholders can prepare for different flood scenarios and implement strategies to minimize impacts on production.

4.3.2 Rate of change in PCLR curves across sectors

PCLR curves for each sector are presented on a single graph, illustrating losses under different inundation depths, as shown in Fig. 6(a). Initially, losses in manufacturing sector are higher than in wholesale and retail trade sector, but they are negligible.

https://doi.org/10.5194/egusphere-2024-3923
Preprint. Discussion started: 27 March 2025

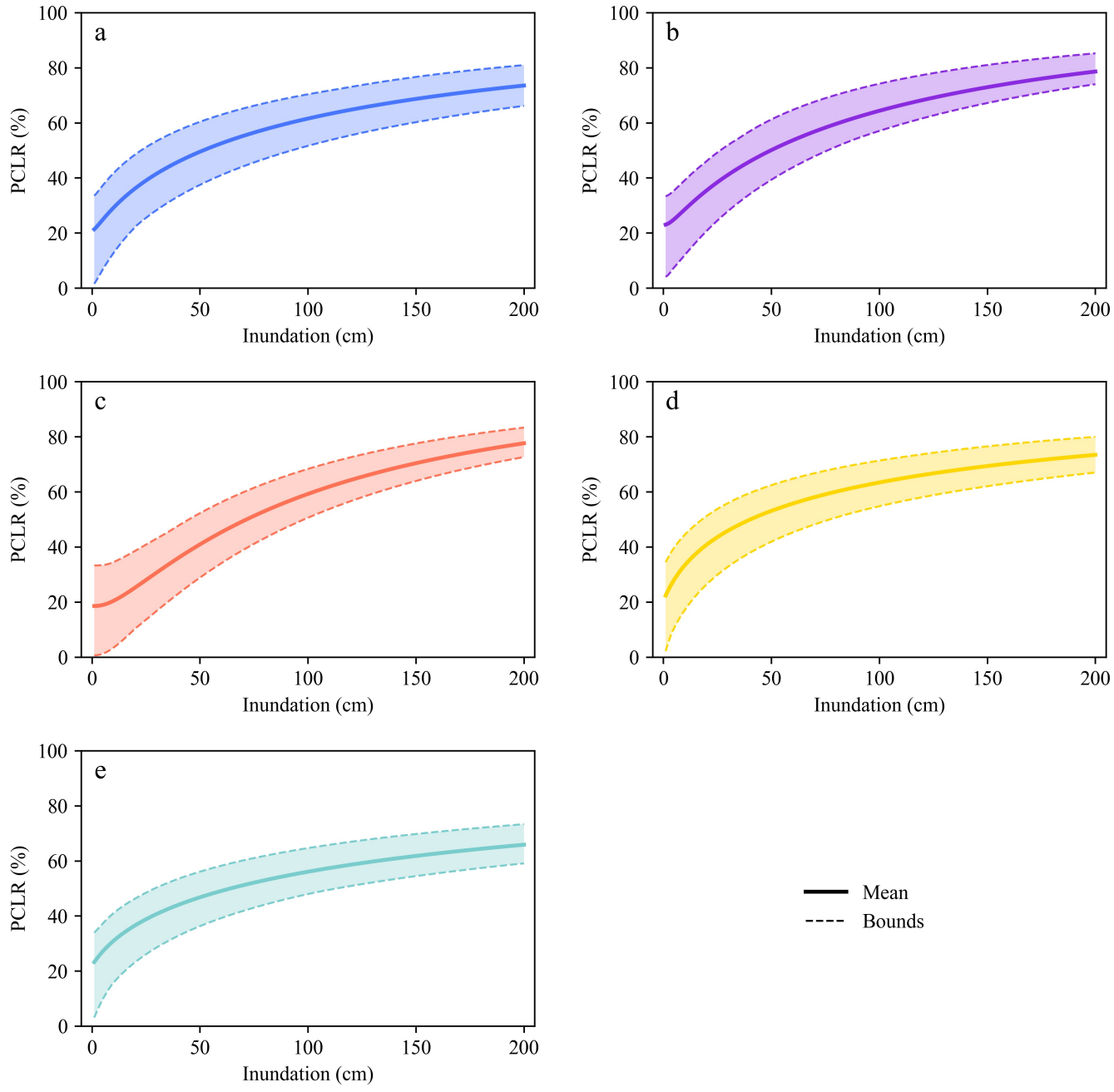

Figure 5. PCLR curves of different sectors. (a) All sectors; (b) manufacturing; (c) accommodation and catering; (d) wholesale and retail trade; (e) other sectors.

https://doi.org/10.5194/egusphere-2024-3923
Preprint. Discussion started: 27 March 2025

For inundation depths below 80 cm, wholesale and retail trade sector incurs the highest losses, followed by manufacturing sector, and accommodation and catering sector experiences the least. Between 80 cm and 130 cm, manufacturing sector suffers the most losses, followed by wholesale and retail trade sector, with accommodation and catering sector still experiencing the least. For depths over 130 cm, manufacturing sector continues to incur the greatest losses, but accommodation and catering sector surpasses wholesale and retail trade sector. These findings show that sector vulnerability varies with flood conditions, highlighting the need for tailored flood risk management strategies.

While PCLR curves show post-disaster losses for each sector, they are limited by their one-dimensional analysis. To improve disaster prevention strategies, this study also estimates the rate of change in PCLR curves for each sector. This rate reflects how quickly losses change with inundation depth under specific conditions. Understanding this rate provides deeper insight into sector-specific vulnerabilities. Fig. 6(b) presents the rate of change in losses across sectors under varying inundation depths. We find that at depths less than 17 cm, wholesale and retail trade sector has a higher rate of change than manufacturing sector and accommodation and catering sector. However, as depth increases, the dynamics shift. Between 17 cm and 27 cm, manufacturing sector shows the highest rate of change, surpassing both wholesale and retail trade sector and accommodation and catering sector. Beyond 27 cm, accommodation and catering sector has the highest rate of loss change, exceeding the manufacturing sector.

At shallow inundation depths, PCLR curve of wholesale and retail trade sector exhibits the steepest slope. This steepness can be attributed to the sector's high reliance on physical location and customer footfall. Even minor flooding can disrupt transportation, affecting customer access and quickly reducing sales. Additionally, inventory losses can also rise rapidly, particularly for water-sensitive goods. As inundation depth increases, manufacturing sector's vulnerability curve becomes steeper than that of wholesale and retail trade sector. This change is related to sector's reliance on infrastructure and production lines. Greater depths increase damage to production and storage facilities, and cause interruptions to electricity and logistics, resulting in faster losses. At even higher depths, accommodation and catering sector's vulnerability curve becomes the steepest. This sector relies heavily on immediate service and customer experience. Flood damage to facilities, hygiene problems, and service interruptions impact operations. Furthermore, worsening floods can increase evacuations from affected areas, decreasing demand for accommodation and catering services.

4.4 Discussion

4.4.1 Advantages and limitations

A methodological framework was proposed to address response bias in assessing PCLR of enterprises caused by flood disasters, and it was applied to Zhengzhou City as a case study. The results indicate that the proposed framework can provide reliable risk assessment for extreme flood disasters. The methodology has the following advantages: (1) It addresses response bias in extreme flood scenarios and considers the distribution characteristics of PCLR under different damage states, allowing for more accurate assessment of direct economic losses amidst the complexity of real-world data. (2) It calculates the prediction intervals for PCLR curves using MCS, providing a basis for decision-makers to allocate funds based on their financial situations.

https://doi.org/10.5194/egusphere-2024-3923
Preprint. Discussion started: 27 March 2025

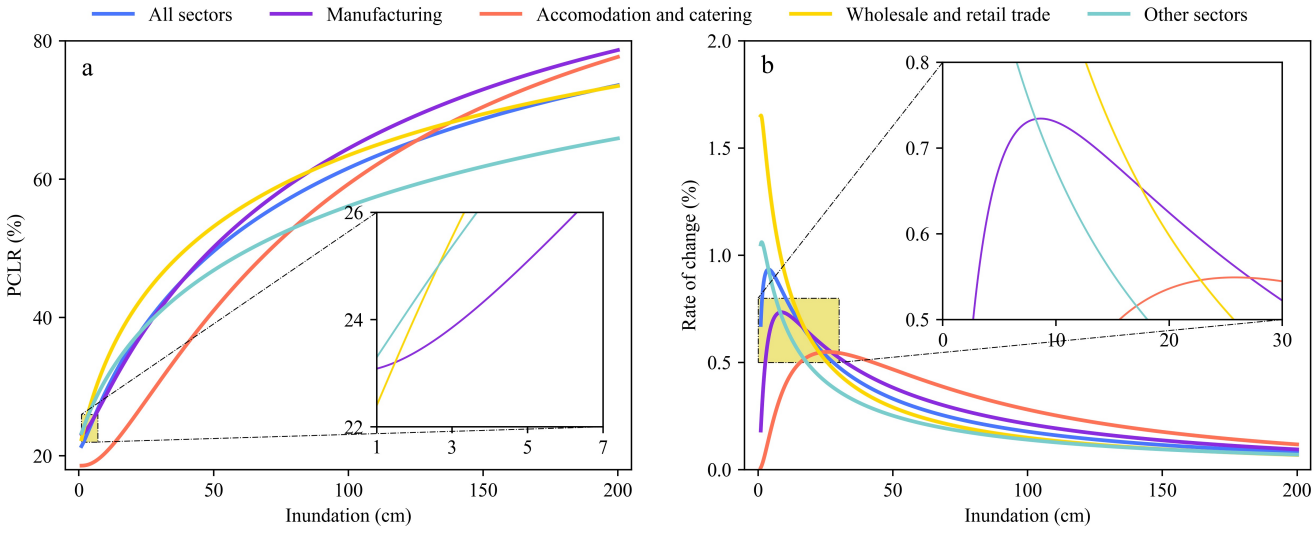

Figure 6. Sectoral PCLR curves and rate of change.

(3) It calculates the rate of change in PCLR with increasing inundation depth, helping emergency managers and businesses understand PCLR sensitivity to rising inundation depth.

The core value of this study lies in the potential application of the estimated PCLR values in economic modeling. These values provide precise supply-side inputs for IO and CGE models. This enhances the accuracy of assessing the ripple effects of production disruptions on the economy, and aids governments in formulating effective response strategies.

However, the proposed approach has some limitations. Although we try to improve model adaptability, the model's generalization ability still requires further validation. Since disasters are unique and unpredictable events, addressing their impacts necessitates specific considerations in modeling (Ribeiro and Pena Jardim Gonçalves, 2019). In addition, how to classify the damage states should also be further discussed.

4.4.2 Future work

Based on this study, future research should focus on several key points.

Firstly, increasing the sample size through on-site investigations should be taken into account when modeling. A multiple dataset can provide a more comprehensive representation of the variability and uncertainty inherent in real-world scenarios (Shooraki et al., 2024). This helps ensure that the model performs consistently well with new and unseen data.

Secondly, incorporating data from diverse regions and sectors is important for enhancing the model's universality. Different regions and sectors have unique factors that influence outcomes (Liu et al., 2012). This study, however, focuses only on manufacturing, accommodation and catering, and wholesale and retail trade in Zhengzhou. Expanding the scope could provide deeper insights into sector-specific dynamics and risk factors. Despite the limitation, this study offers a foundational understanding that can be built upon in subsequent studies.

https://doi.org/10.5194/egusphere-2024-3923
Preprint. Discussion started: 27 March 2025

Finally, numerous studies classify damage states without considering whether different classification methods affect result robustness (Pnevmatikos et al., 2019; Petala et al., 2024). This neglect may lead to a misinterpretation of damage states, resulting in inaccurate assessments and decision-making errors (Gaetani d'Aragona et al., 2024). Thus, future research could focus on classifying damage states, such as dividing PCLR into 3, 4, 5 and more categories, to determine the robustness of results across different classifications.

4.4.3 Measures of flood disaster

This study indicates differences in the severity and rate of change of PCLR curves across sectors due to floods. Therefore, it is crucial to adopt targeted flood risk management strategies to enhance disaster resilience within each sector.

Firstly, government should focus on strengthening infrastructure, particularly in regions with manufacturing sector and wholesale and retail trade sector. Since these sectors highly depend on infrastructure, investments should aim to improve and reinforce roads, power supplies, and logistics networks to mitigate the indirect impacts of flooding. Secondly, for accommodation and catering sector, detailed emergency response plans and recovery strategies need to be developed. As this sector experiences the greatest variability in PCLR during severe flooding, policymakers should promote the establishment of sector-specific emergency fund. This fund would provide financial support and short-term loans to assist businesses in recovering quickly after a disaster. Lastly, it is recommended that the government establish a multi-sector collaboration mechanism to ensure rapid response and coordinated action among relevant departments when disasters occur. By creating an information-sharing platform, businesses and government agencies across sectors can access up-to-date flood information promptly, allowing for more informed decision-making in response efforts.

5 Conclusions

This study addresses the challenge of estimating mean PCLR after extreme disaster events, a significant issue in disaster research. By constructing exceedance probability curves and employing distribution function fitting, we develop a method to estimate mean PCLR considering response bias. The application of MCS further enhances the reliability of our estimates by providing prediction intervals, which are essential for guiding post-disaster government resource allocation. Additionally, we calculate the rate of change of PCLR to understand the sensitivity of sector-specific PCLR to varying inundation depths. Then, the proposed method is applied to 424 data samples collected after the Zhengzhou rainstorm event in July 2021. The estimated PCLR values can serve as a driving condition in IO and CGE models, allowing for a more accurate estimation of the ripple effects of flood losses.

This study identifies key patterns in sectoral losses in relation to inundation depths. Losses are most severe in wholesale and retail trade sector at shallower depths. At moderate and greater depths, manufacturing experiences the highest losses. The rate of change in PCLR differs significantly between sectors. Wholesale and retail trade sector is most sensitive at minimal depths. Manufacturing is most sensitive at moderate depths, while accommodation and catering sector shows the highest sensitivity at greater depths. These findings highlight the importance of directing support to the most affected sectors, especially

https://doi.org/10.5194/egusphere-2024-3923
Preprint. Discussion started: 27 March 2025

manufacturing and wholesale and retail trade, to reduce economic disruption. The varying sensitivity of sectors to inundation should guide policy-making due to its impact on economic and social resilience.

As climate changes, the frequency and severity of natural disasters such as floods, hurricanes, and rising sea levels are expected to increase. This research offers an insight for policymakers in disaster management, allowing for the strategic allocation of limited resources and the accurate ripple effect estimation. Given access to primary data on hazard intensity and PCLR, the analytical model in this study can be adapted to the characteristics of different regions and sectors. It is applicable in various disaster scenarios, providing a tool for managing future economic challenges.

Data availability. Data will be made available on request.

Author contributions. Lijiao Yang: conceptualization, methodology, writing-review and editing, funding acquisition, resources, supervision. Yan Luo: conceptualization, methodology, formal analysis, writing-original draft preparation, writing-review and editing. Zilong Li: conceptualization, methodology, formal analysis, visualization. Xinyu Jiang: conceptualization, methodology, formal analysis and investigation, writing-review and editing, funding acquisition, resources.

Competing interests. The authors declare that none of the authors has any competing interests.

https://doi.org/10.5194/egusphere-2024-3923
Preprint. Discussion started: 27 March 2025

References

Andreotti, G. and Lai, C.: Use of fragility curves to assess the seismic vulnerability in the risk analysis of mountain tunnels, Tunn. Undergr. Space Technol., 91, https://doi.org/10.1016/j.tust.2019.103008, 2019.

Asche, F., Anderson, J. L., Botta, R., Kumar, G., Abrahamsen, E. B., Nguyen, L. T., and Valderrama, D.: The economics of shrimp disease, J. Invertebr. Pathol., 186, https://doi.org/10.1016/j.jip.2020.107397, 2021.

Baker, J. W.: Efficient Analytical Fragility Function Fitting Using Dynamic Structural Analysis, Earthq. Spectra, 31, 579–599, https://doi.org/10.1193/021113eqs025m, 2015.

Borga, M., Comiti, F., Ruin, I., and Marra, F.: Forensic analysis of flash flood response, WIREs Water, 6, https://doi.org/10.1002/wat2.1338, 2019.

Botzen, W. J. W., Deschenes, O., and Sanders, M.: The Economic Impacts of Natural Disasters: A Review of Models and Empirical Studies, Rev. Environ. Econ. Policy, 13, 167–188, https://doi.org/10.1093/reep/rez004, 2019.

Brusset, X., Ivanov, D., Jebali, A., La Torre, D., and Repetto, M.: A dynamic approach to supply chain reconfiguration and ripple effect analysis in an epidemic, Int. J. Prod. Econ., 263, https://doi.org/10.1016/j.ijpe.2023.108935, 2023.

Burton, H. V., Deierlein, G., Lallemant, D., and Lin, T.: Framework for Incorporating Probabilistic Building Performance in the Assessment of Community Seismic Resilience, J. Struct. Eng., 142, https://doi.org/10.1061/(ASCE)ST.1943-541X.0001321, 2016.

Cabrera, T., Hube, M. A., María, H. S., Silva, V., Martins, L., Yepes-Estrada, C., and Chacón, M. F.: Empirical fragility curves for houses in Chile using damage data from two earthquakes, Bull. Earthq. Eng., 22, 5619–5638, https://doi.org/10.1007/s10518-024-01933-w, 2024.

Cai, M. and Wei, G.: A fuzzy social vulnerability evaluation from the perception of disaster bearers against meteorological disasters, Nat. Hazards, 103, 2355–2370, https://doi.org/10.1007/s11069-020-04088-4, 2020.

Carrera, L., Standardi, G., Bosello, F., and Mysiak, J.: Assessing direct and indirect economic impacts of a flood event through the integration of spatial and computable general equilibrium modelling, Environ. Modell. Software, 63, 109–122, https://doi.org/10.1016/j.envsoft.2014.09.016, 2015.

Choi, E., DesRoches, R., and Nielson, B.: Seismic fragility of typical bridges in moderate seismic zones, Eng. Struct., 26, 187–199, https://doi.org/10.1016/j.engstruct.2003.09.006, 2004.

Christensen, A. P., Garrido, L. E., Guerra-Peña, K., and Golino, H.: Comparing community detection algorithms in psychometric networks: A Monte Carlo simulation, Behav. Res. Methods, 56, 1485–1505, https://doi.org/10.3758/s13428-023-02106-4, 2024.

Dong, B., Xia, J., Li, Q., and Zhou, M.: Risk assessment for people and vehicles in an extreme urban flood: Case study of the “7.20” flood event in Zhengzhou, China, Int. J. Disaster Risk Reduct., 80, https://doi.org/10.1016/j.ijdrr.2022.103205, 2022.

EMDAT: 2023 Disasters in Numbers: A Significant Year of Disaster Impact, https://files.emdat.be/reports/2023_EMDAT_report.pdf, 2024.

Gaetani d’Aragona, M., Polese, M., and Prota, A.: Seismic fragility curves for infilled RC building classes considering multiple sources of uncertainty, Eng. Struct., 321, https://doi.org/10.1016/j.engstruct.2024.118888, 2024.

Gertz, A. B., Davies, J. B., and Black, S. L.: A CGE Framework for Modeling the Economics of Flooding and Recovery in a Major Urban Area, Risk Anal., 39, 1314–1341, https://doi.org/10.1111/risa.13285, 2019.

Goda, K., Yasuda, T., Mori, N., Muhammad, A., De Risi, R., and De Luca, F.: Uncertainty quantification of tsunami inundation in Kuroshio, Kochi Prefecture, Japan, using the Nankai–Tonankai megathrust rupture scenarios, Natural Hazards and Earth System Sciences, 20, 3039–3056, https://doi.org/10.5194/nhess-20-3039-2020, 2020.

https://doi.org/10.5194/egusphere-2024-3923
Preprint. Discussion started: 27 March 2025

Hallegatte, S., Green, C., Nicholls, R. J., and Corfee-Morlot, J.: Future flood losses in major coastal cities, Nat. Clim. Change, 3, 802–806, https://doi.org/10.1038/nclimate1979, 2013.

Hariri-Ardebili, M. and Saouma, V.: Probabilistic seismic demand model and optimal intensity measure for concrete dams, Struct. Saf., 59, 67–85, https://doi.org/10.1016/j.strusafe.2015.12.001, 2016.

Heo, S., Lim, J. Y., Chang, R., Shim, Y., Ifaei, P., and Yoo, C.: Non-Gaussian multivariate statistical monitoring of spatio-temporal wind speed frequencies to improve wind power quality in South Korea, J. Environ. Manage., 318, https://doi.org/10.1016/j.jenvman.2022.115516, 2022.

Hung, Y.-H., Li, L. Y., and Cheng, T.: Uncovering hidden capacity in overall equipment effectiveness management, Int. J. Prod. Econ., 248, https://doi.org/10.1016/j.ijpe.2022.108494, 2022.

IPCC: Summary for Policymakers, https://www.ipcc.ch/report/ar6/syr/, 2023.

Jiang, X., Mori, N., Tatano, H., Yang, L., and Shibutani, Y.: Estimation of property loss and business interruption loss caused by storm surge inundation due to climate change: a case of Typhoon Vera revisit, Nat. Hazards, 84, 35–49, https://doi.org/10.1007/s11069-015-2085-z, 2015.

Jiang, X., Lin, Y., and Yang, L.: A simulation-based approach for assessing regional and industrial flood vulnerability using mixed-MRIO model: A case study of Hubei Province, China, J. Environ. Manage., 339, https://doi.org/10.1016/j.jenvman.2023.117845, 2023.

Kajitani, Y. and Tatano, H.: ESTIMATION OF PRODUCTION CAPACITY LOSS RATE AFTER THE GREAT EAST JAPAN EARTHQUAKE AND TSUNAMI IN 2011, Econ. Syst. Res., 26, 13–38, https://doi.org/10.1080/09535314.2013.872081, 2014.

Kajitani, Y. and Tatano, H.: Applicability of a spatial computable general equilibrium model to assess the short-term economic impact of natural disasters, Econ. Syst. Res., 30, 289–312, https://doi.org/10.1080/09535314.2017.1369010, 2018.

Karmakar, D., Ray-Chaudhuri, S., and Shinozuka, M.: Finite element model development, validation and probabilistic seismic performance evaluation of Vincent Thomas suspension bridge, Struct. Infrastruct. Eng., 11, 223–237, https://doi.org/10.1080/15732479.2013.863360, 2015.

Kaur, H., Singh, S. P., Garza-Reyes, J. A., and Mishra, N.: Sustainable stochastic production and procurement problem for resilient supply chain, Comput. Ind. Eng., 139, https://doi.org/10.1016/j.cie.2018.12.007, 2020.

Kayaga, S. M., Amankwaa, E. F., Gough, K. V., Wilby, R. L., Abarike, M. A., Codjoe, S. N. A., Kasei, R., Nabilse, C. K., Yankson, P. W. K., Mensah, P., Abdullah, K., and Griffiths, P.: Cities and extreme weather events: impacts of flooding and extreme heat on water and electricity services in Ghana, Environ. Urban., 33, 131–150, https://doi.org/10.1177/0956247820952030, 2021.

Koks, E. E. and Thissen, M.: A Multiregional Impact Assessment Model for disaster analysis, Econ. Syst. Res., 28, 429–449, https://doi.org/10.1080/09535314.2016.1232701, 2016.

Koks, E. E., Bočkarjova, M., de Moel, H., and Aerts, J. C. J. H.: Integrated Direct and Indirect Flood Risk Modeling: Development and Sensitivity Analysis, Risk Anal., 35, 882–900, https://doi.org/10.1111/risa.12300, 2015.

Koks, E. E., Carrera, L., Jonkeren, O., Aerts, J. C. J. H., Husby, T. G., Thissen, M., Standardi, G., and Mysiak, J.: Regional disaster impact analysis: comparing input–output and computable general equilibrium models, Nat. Hazard. Earth Sys., 16, 1911–1924, https://doi.org/10.5194/nhess-16-1911-2016, 2016.

Lenzen, M., Malik, A., Kenway, S., Daniels, P., Lam, K. L., and Geschke, A.: Economic damage and spillovers from a tropical cyclone, Natural Hazards and Earth System Sciences, 19, 137–151, https://doi.org/10.5194/nhess-19-137-2019, 2019.

https://doi.org/10.5194/egusphere-2024-3923
Preprint. Discussion started: 27 March 2025

Lima, A. O., Lyra, G. B., Abreu, M. C., Oliveira-Júnior, J. F., Zeri, M., and Cunha-Zeri, G.: Extreme rainfall events over Rio de Janeiro State, Brazil: Characterization using probability distribution functions and clustering analysis, Atmos. Res., 247, https://doi.org/10.1016/j.atmosres.2020.105221, 2021.

Liu, H., Tatano, H., Kajitani, Y., and Yang, Y.: Analysis of the influencing factors on industrial resilience to flood disasters using a semi-Markov recovery model: A case study of the Heavy Rain Event of July 2018 in Japan, Int. J. Disaster Risk Reduct., 82, https://doi.org/10.1016/j.ijdrr.2022.103384, 2022a.

Liu, H., Tatano, H., Kajitani, Y., and Yang, Y.: Methodology for estimating regional production capacity loss rate in industrial sectors caused by disasters: A case study of the 2016 Kumamoto earthquakes, Int. J. Disaster Risk Reduct., 110, https://doi.org/10.1016/j.ijdrr.2024.104631, 2024.

Liu, X., Wu, J., Zhang, S., Wang, Z., and Garg, H.: Extended Cumulative Residual Entropy for Emergency Group Decision-Making Under Probabilistic Hesitant Fuzzy Environment, Int. J. Fuzzy Syst., 24, 159–179, https://doi.org/10.1007/s40815-021-01122-w, 2022b.

Liu, Z., Geng, Y., Lindner, S., and Guan, D.: Uncovering China's greenhouse gas emission from regional and sectoral perspectives, Energy, 45, 1059–1068, https://doi.org/10.1016/j.energy.2012.06.007, 2012.

Lv, H., Wu, Z., Zheng, X., Yan, D., Yu, Z., and Shang, W.: Multi-attribute diagnosis of urban flood-bearing bodies based on integrated learning with Stacking–GPR–QPSO coupling, J. Hydrol., 645, https://doi.org/10.1016/j.jhydrol.2024.132222, 2024.

Moccia, B., Mineo, C., Ridolfi, E., Russo, F., and Napolitano, F.: Probability distributions of daily rainfall extremes in Lazio and Sicily, Italy, and design rainfall inferences, J. Hydrol. Reg. Stud., 33, https://doi.org/10.1016/j.ejrh.2020.100771, 2021.

Nakano, K., Kajitani, Y., and Tatano, H.: FUNCTIONAL FRAGILITY CURVES FOR A PRODUCTION FACILITY OF INDUSTRIAL SECTORS IN CASE OF EARTHQUAKE DISASTER, Journal of Japan Society of Civil Engineers, Ser. A1 (Structural Engineering & Earthquake Engineering (SE/EE)), 69, 57–68, https://doi.org/10.2208/jscejseee.69.57, 2013.

Nguyen, H. D., Kim, C., Lee, Y.-J., and Shin, M.: Incorporation of machine learning into multiple stripe seismic fragility analysis of reinforced concrete wall structures, J. Build. Eng., 97, https://doi.org/10.1016/j.jobe.2024.110772, 2024.

Okuyama, Y. and Santos, J. R.: DISASTER IMPACT AND INPUT-OUTPUT ANALYSIS, Econ. Syst. Res., 26, 1–12, https://doi.org/10.1080/09535314.2013.871505, 2014.

Padgett, J. E. and DesRoches, R.: Methodology for the development of analytical fragility curves for retrofitted bridges, Earthq. Eng. Struct. Dyn., 37, 1157–1174, https://doi.org/10.1002/eqe.801, 2008.

Peng, J. and Zhang, J.: Urban flooding risk assessment based on GIS- game theory combination weight: A case study of Zhengzhou City, Int. J. Disaster Risk Reduct., 77, https://doi.org/10.1016/j.ijdrr.2022.103080, 2022.

Petala, E., Sotiriadis, D., and Klimis, N.: Assessment of fragility curves of highway embankments due to underlying faults rupture propagation, Soil Dyn. Earthq. Eng., 184, https://doi.org/10.1016/j.soildyn.2024.108818, 2024.

Pnevmatikos, N. G., Papagiannopoulos, G. A., and Papavasileiou, G. S.: Fragility curves for mixed concrete/steel frames subjected to seismic excitation, Soil Dyn. Earthq. Eng., 116, 709–713, https://doi.org/10.1016/j.soildyn.2018.09.037, 2019.

Prasad, G. G. and Banerjee, S.: The Impact of Flood-Induced Scour on Seismic Fragility Characteristics of Bridges, J. Earthq. Eng., 17, 803–828, https://doi.org/10.1080/13632469.2013.771593, 2013.

Ribeiro, P. J. G. and Pena Jardim Gonçalves, L. A.: Urban resilience: A conceptual framework, Sustain. Cities Soc., 50, https://doi.org/10.1016/j.scs.2019.101625, 2019.

Shinozuka, M., Feng, M. Q., Lee, J., and Naganuma, T.: Statistical Analysis of Fragility Curves, J. Eng. Mech., 126, 1224–1231, https://doi.org/10.1061/(ASCE)0733-9399(2000)126:12(1224), 2000.

https://doi.org/10.5194/egusphere-2024-3923
Preprint. Discussion started: 27 March 2025

Shooraki, M. K., Bastami, M., Abbasnejadfard, M., and Motamed, H.: Development of seismic fragility curves for hospital buildings using empirical damage observations, Int. J. Disaster Risk Reduct., 108, https://doi.org/10.1016/j.ijdrr.2024.104525, 2024.

Sun, Y., Liu, S., Wang, P., Jian, X., Liao, X., and Chen, W.-Q.: China's roadmap to plastic waste management and associated economic costs, J. Environ. Manage., 309, https://doi.org/10.1016/j.jenvman.2022.114686, 2022.

Tan, R., Zhang, W., and Yang, L.: Decision-making method based on set pair analysis and VIKOR under heterogeneous information environment and application to typhoon disaster assessment, Soft Comput., 27, 8289–8314, https://doi.org/10.1007/s00500-022-07750-0, 2023.

Tatano, H. and Kajitani, Y., eds.: Methodologies for Estimating the Economic Impacts of Natural Disasters, Springer Singapore, https://doi.org/10.1007/978-981-16-2719-4, 2022.

Torbol, M. and Shinozuka, M.: Effect of the angle of seismic incidence on the fragility curves of bridges, Earthq. Eng. Struct. Dyn., 41, 2111–2124, https://doi.org/10.1002/eqe.2197, 2012.

UNDRR: Sendai Framework for Disaster Risk Reduction 2015-2030, https://www.undrr.org/publication/sendai-framework-disaster-risk-reduction-2015-2030, 2015.

Vergeynst, L. L., Dierick, M., Bogaerts, J. A. N., Cnudde, V., and Steppe, K.: Cavitation: a blessing in disguise? New method to establish vulnerability curves and assess hydraulic capacitance of woody tissues, Tree Physiol., 35, 400–409, https://doi.org/10.1093/treephys/tpu056, 2015.

Wei, Y.-M., Wang, K., Wang, Z.-H., and Tatano, H.: Vulnerability of infrastructure to natural hazards and climate change in China, Nat. Hazards, 75, 107–110, https://doi.org/10.1007/s11069-014-1432-9, 2015.

Yang, L., Kajitani, Y., Tatano, H., and Jiang, X.: A methodology for estimating business interruption loss caused by flood disasters: insights from business surveys after Tokai Heavy Rain in Japan, Nat. Hazards, 84, 411–430, https://doi.org/10.1007/s11069-016-2534-3, 2016.

Yang, L., Wang, X., Jiang, X., and Tatano, H.: Assessing the Regional Economic Ripple Effect of Flood Disasters Based on a Spatial Computable General Equilibrium Model Considering Traffic Disruptions, Int. J. Disaster Risk Sci., 14, 488–505, https://doi.org/10.1007/s13753-023-00500-2, 2023.

Yang, Y., Chen, G., and Reniers, G.: Vulnerability assessment of atmospheric storage tanks to floods based on logistic regression, Reliab. Eng. Syst. Saf., 196, https://doi.org/10.1016/j.ress.2019.106721, 2020.

Yin, J., Yu, D., Yin, Z., Liu, M., and He, Q.: Evaluating the impact and risk of pluvial flash flood on intra-urban road network: A case study in the city center of Shanghai, China, J. Hydrol., 537, 138–145, https://doi.org/10.1016/j.jhydrol.2016.03.037, 2016.

Zentner, I., Gündel, M., and Bonfils, N.: Fragility analysis methods: Review of existing approaches and application, Nucl. Eng. Des., 323, 245–258, https://doi.org/10.1016/j.nucengdes.2016.12.021, 2017.

Zhang, H., Fang, W., Zhang, H., and Yu, L.: Assessment of direct economic losses of flood disasters based on spatial valuation of land use and quantification of vulnerabilities: a case study on the 2014 flood in Lishui city of China, Natural Hazards and Earth System Sciences, 21, 3161–3174, https://doi.org/10.5194/nhess-21-3161-2021, 2021.